

## Accumulation of Atmospheric Mercury in Glacier Cryoconite over Western China

Jie Huang,<sup>\*,†,§,ID</sup> Shichang Kang,<sup>‡,§,◇</sup> Ming Ma,<sup>||</sup> Junming Guo,<sup>‡</sup> Zhiyuan Cong,<sup>†,§,ID</sup> Zhiwen Dong,<sup>‡</sup> Runsheng Yin,<sup>⊥</sup> Jianzhong Xu,<sup>‡,ID</sup> Lekhendra Tripathee,<sup>‡</sup> Kirpa Ram,<sup>‡,#</sup> and Feiyue Wang<sup>∇,ID</sup>

<sup>†</sup>Key Laboratory of Tibetan Environment Changes and Land Surface Processes, Institute of Tibetan Plateau Research and <sup>§</sup>CAS Center for Excellence in Tibetan Plateau Earth Sciences, Chinese Academy of Sciences, Beijing 100101, China

<sup>‡</sup>State Key Laboratory of Cryospheric Science, Northeast Institute of Eco-Environment and Resources, Chinese Academy of Sciences, Lanzhou 730000, China

<sup>||</sup>College of Resources and Environment, Southwest University, Chongqing 400715, China

<sup>⊥</sup>State Key Laboratory of Ore Deposit Geochemistry, Institute of Geochemistry, Chinese Academy of Sciences, Guiyang, 550002, China

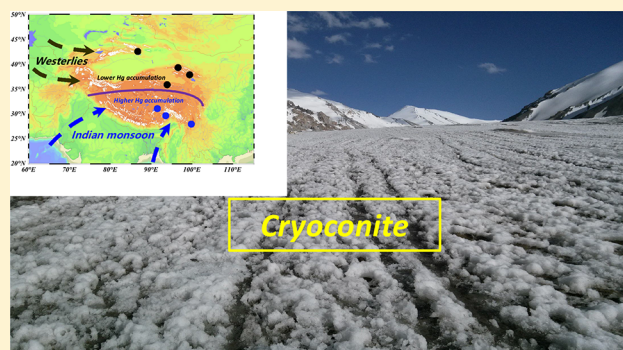
<sup>#</sup>Institute of Environment and Sustainable Development, Banaras Hindu University, Varanasi, 221005, India

<sup>∇</sup>Center for Earth Observation Science, and Department of Environment and Geography, University of Manitoba, Winnipeg, Manitoba R3T 2N2, Canada

<sup>◇</sup>University of the Chinese Academy of Sciences, Beijing 100049, China

### S Supporting Information

**ABSTRACT:** Cryoconite is a granular aggregate, comprised of both mineral and biological material, and known to accumulate atmospheric contaminants. In this study, cryoconite was sampled from seven high-elevation glaciers in Western China to investigate the spatial and altitudinal patterns of atmospheric mercury (Hg) accumulation in the cryoconite. The results show that total Hg ( $Hg_T$ ) concentrations in cryoconite were significant with relatively higher Hg accumulation in the southern glaciers ( $66.0 \pm 29.3 \text{ ng g}^{-1}$ ), monsoon-influenced regions, than those in the northern glaciers ( $42.5 \pm 20.7 \text{ ng g}^{-1}$ ), westerlies-influenced regions. The altitudinal profile indicates that  $Hg_T$  concentrations in the northern glaciers decrease significantly with altitude, while those in the southern glaciers generally increase toward higher elevations. Unexpectedly high accumulation of methyl-Hg (MeHg) with an average of  $1.0 \pm 0.4 \text{ ng g}^{-1}$  was also detected in the cryoconite samples, revealing the surface of cryoconite could act as a potential site for Hg methylation in alpine environments. Our preliminary estimate suggests a storage of  $\sim 34.3 \pm 17.4$  and  $0.65 \pm 0.28 \text{ kg}$  of  $Hg_T$  and MeHg from a single year of formation process in the glacier cryoconite. Therefore, glacier cryoconite could play an important role in Hg storage and transformation, which may result in downstream effects on glacier-fed ecosystems under climate warming scenario.



## INTRODUCTION

Cryoconite is a granular aggregate of mineral and organic materials that are commonly found on glacier surfaces.<sup>1</sup> Cryoconite present in melting snow or ice tends to stay on site and forms an increasingly dense layer on glacier surfaces, which is responsible for the dark or “dirty” appearance of alpine glaciers during the ablation season (Figure S1, Supporting Information). As cryoconite can absorb solar radiation more efficiently than the surrounding snow/ice surfaces, its role in reducing the albedo of glaciers and increasing glacier melting has been well recognized.<sup>2,3</sup> Cryoconite is also known to accumulate atmospheric contaminants such as mercury (Hg) onto extracellular polymeric substances secreted by cryoconite

microorganisms,<sup>4–6</sup> the extent for which this occurs to Hg is the main focus of this study.

Hg is a contaminant of primary concern in the global environment, including atmosphere, glaciers, and lakes, etc., due to its high toxicity to biota.<sup>7</sup> The organic form of Hg, methyl-Hg (MeHg), biomagnifies in the aquatic ecosystems and is a known developmental neurotoxin to humans.<sup>8</sup> Owing to its high toxicity, anthropogenic emissions of Hg have been

Received: November 21, 2018

Revised: May 20, 2019

Accepted: May 21, 2019

Published: May 22, 2019

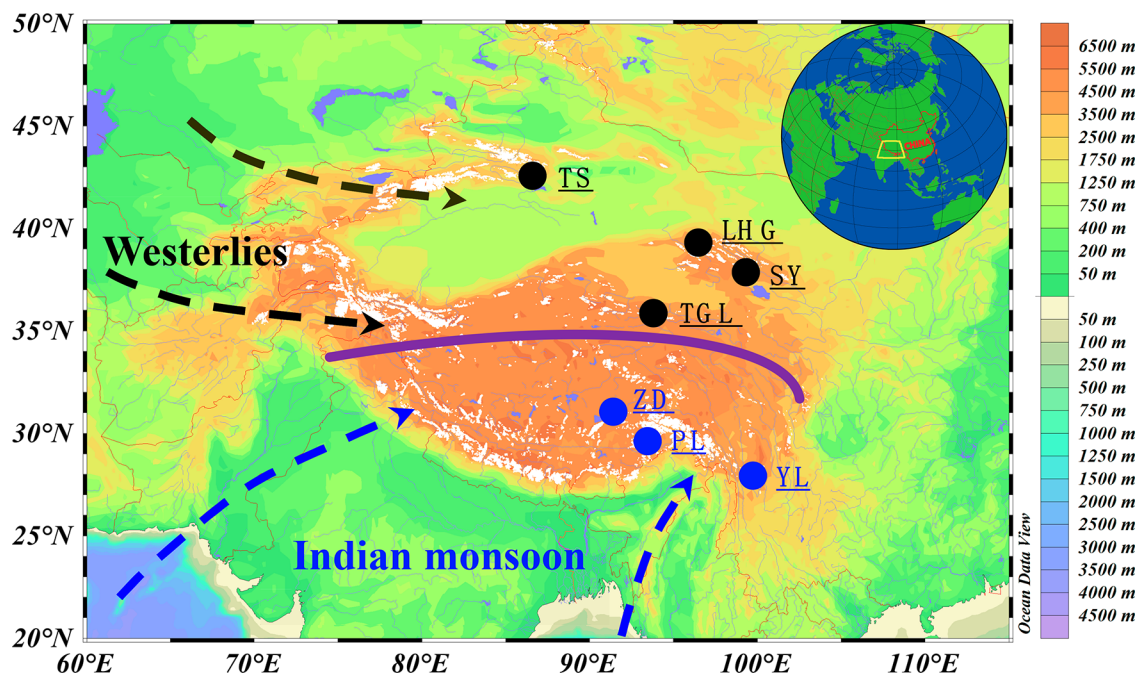


**Figure 1.** Locations of the glaciers in Western China where cryoconite samples were collected (acronyms are TS, Urumqi No. 1 Glacier; LHG, Laohugou No. 12 Glacier; SY, Shiyi Glacier; TGL, Dongkemadi Glacier; ZD, Zhadong Glacier; PL, Parlung No. 4 Glacier; YL, Yulong Glacier). Purple line shows the northern boundary of the Indian monsoon based on seasonal changes in  $\delta^{18}\text{O}$  of precipitation on the Tibetan Plateau.

increasingly regulated with the recently signed Minamata Convention that entered into force in 2017.<sup>9</sup> Long-range atmospheric transport is primarily responsible for the transport of Hg to remote ecosystems in high latitudes<sup>10,11</sup> and altitudes,<sup>12,13</sup> where it can be deposited and accumulated in cryospheric environments such as glaciers. As a result of the global warming, glaciers and ice caps are largely experiencing a shrinkage worldwide.<sup>14,15</sup> The accumulated Hg in the cryoconite can be released during melting of glaciers and thus may additionally contribute for contamination of the downstream ecosystems in these regions.

Western China, defined herein as the Tibetan Plateau and the Xinjiang Uyghur Autonomous Region of China, is the most snow/ice concentrated area outside the polar regions. There were a total of 42 370 glaciers covering 43 087 km<sup>2</sup> in Western China,<sup>16</sup> which accounts for 21.4% (by the number) and 5.9% (by area coverage) of global glaciers in the Randolph Glacier Inventory.<sup>17</sup> Western China is also known as the “Water Tower of Asia” since glacier meltwater from this region is the major source of freshwater for more than one-third of the world’s population.<sup>18</sup> While much of Western China is highly isolated and inaccessible, it is surrounded by rapidly industrializing countries of South and Central Asia (Figure 1). Anthropogenic contaminants such as Hg released from these countries can migrate to Western China via long-range atmospheric transport, which has greatly altered its previously pristine interior alpine ecosystems.<sup>19–21</sup> As a result of transboundary air pollution, the deposition rates of atmospheric Hg over the Tibetan Plateau have been shown to be up to seven times higher in the post-World War II period than those in the pre-Industrial era.<sup>21</sup>

Since atmospheric deposition of Hg in Western China is dominated by Hg bound to particulates,<sup>12,22,23</sup> it is possible that atmospheric Hg deposition to glaciers is accumulated in cryoconite. As cryoconite is one of the most biologically active habitats within glacial ecosystems,<sup>1,24,25</sup> it is also possible that

Hg methylation, a primarily microbially mediated process converting inorganic Hg to MeHg, may occur in cryoconite. However, to our best knowledge, only a few studies on the distribution and fate of Hg in glacier cryoconite have been reported,<sup>26</sup> thus reflecting a knowledge gap in our understanding of biogeochemical Hg cycling in the global cryosphere in a changing climate. Here we present the first study on the geographical, both spatial and altitudinal, distribution of Hg in glacier cryoconite in Western China. We also intended to understand the distribution patterns of Hg and its accumulation in glacier cryoconite related to major climatic and environmental variables and to evaluate the temporary storage and possible release of Hg in the alpine glacier reservoir.

## ■ MATERIALS AND METHODS

**Study Area and Sample Collection.** The geography of Western China is characterized by the Tibetan Plateau (mean elevation > 4000 m a.s.l.) in the south and vast deserts in the north (Figure 1). The large-scale atmospheric circulation patterns over Western China are mainly influenced by the westerlies in winter and the Indian monsoon in summer,<sup>27</sup> resulting in two main climatic zones (monsoon-influenced region in the south and westerlies-influenced region in the north) according to seasonal changes in atmospheric circulation (Figure 1).

The cryoconite is generally found below 5 cm on the glacier surfaces in Western China,<sup>28</sup> and cryoconite is treated as a solid sample<sup>4–6</sup> since it has a low content of snow/ice component (Figure S1, Supporting Information). A total of 48 cryoconite samples were randomly collected from seven high-altitude glaciers in Western China. These glaciers include the Urumqi No. 1 Glacier (TS) in the Tianshan Mountains, Laohugou No. 12 Glacier (LHG) and Shiyi Glacier (SY) in the Qilian Mountains, Dongkemadi Glacier (TGL) in the Tanggula Mountains, Zhadong Glacier (ZD) in the Nyainqentanglha Mountains, Parlung No. 4 Glacier (PL) in

Table 1. Details of the Cryoconite Samples and the Glaciers from Where They Were Collected

site	glacier	location	glacier area (km <sup>2</sup> )	longitude, latitude	N	sampling date	equilibrium line altitude (m a.s.l.)	annual precipitation (mm)
TS	Urumqi Glacier No. 1	Tienshan Mountains	1.7	43°07'N, 86°48'E	13	Sep 3, 2014	4168	255
LHG	Laohugou Glacier No. 12	Qilian Mountains	21.9	39°26'N, 96°33'E	14	Jul 29, 2014 and Aug 8, 2014	4900	52
SY	Shiyi Glacier	Qilian Mountains	0.5	38°21'N, 99°88'E	4	Aug 12, 2012	>4320	162
TGL	Dongkemadi Glacier	Tanggula Mountains	1.7	33°04'N, 92°04'E	4	Aug 10, 2014	5720	264
ZD	Zhadang Glacier	Nyainqêntanglha Mountains	2.0	30°29'N, 96°55'E	2	Aug 8, 2016	6024	539
PL	Parlung Glacier No. 4	Eastern Himalayas	6.9	29°14'N, 90°38'E	2	Jul 26, 2014	5424	827
YL	Baishui Glacier No. 1	Hengduan Mountains	1.3	27°18'N, 100°08'E	9	May 20, 2014	4972	855

the eastern Himalayas, and Yulong Glacier (Baishui No. 1 Glacier) (YL) in the Hengduan Mountains (Figure 1 and Table 1). All of these glaciers are located in extremely remote areas that are difficult to access but represent a broad range of cryoconite deposition on the glaciers of Western China. Most of the samples were collected from July to September 2014, except for SY which was collected in August 2012 and ZD in August 2016. Cryoconite samples were collected from the superimposed glacier surfaces in the ablation zones with a precleaned stainless-steel shovel and stored in amber glass bottles (Nalgene). Before collecting the next sample, the shovel and other sampling devices were cleaned by low hydrochloric acid (0.1% v/v) and ultrapure water in the field in order to avoid possible contaminations from the previous sample. All samples were kept frozen until they were transported to the state key laboratory of cryospheric science, Chinese Academy of Sciences, for analysis. Further information about the study area and sampling can be found in Text S1 of the Supporting Information.

**Analytical Procedures and QA/QC.** After collection, cryoconite samples were freeze dried at  $-70\text{ }^{\circ}\text{C}$ ; total Hg ( $\text{Hg}_T$ ) concentrations in the cryoconite ( $\sim 0.2\text{ g}$  of sample) were determined on a Leeman Hydra-II<sub>C</sub> direct Hg analyzer (Teledyne Leeman Laboratories, Hudson, NH), which involves thermal decomposition and detection by atomic absorption spectroscopy, following the US EPA Method 7473. The method detection limit (MDL), defined as 3 times the standard deviation of 10 replicate measurements of sample blanks, was  $0.06\text{ ng g}^{-1}$ . The reproducibility, reported as relative percentage deviations (RPDs) for the replicate samples, was  $<5\%$ . The accuracy of measurement was assessed by measuring Chinese geochemical standard reference material GSS-9 (lake sediment,  $[\text{Hg}] = 32\text{ ng g}^{-1}$ , from the China National Center for Standard Reference Materials) and was found to be less than  $5\%$  (RPDs). The recoveries of GSS-9 standard reference material for  $\text{Hg}_T$  measurements were in the range of  $98\text{--}103\%$ .

MeHg concentrations in the cryoconite were determined following the procedures of Liang et al.,<sup>29</sup> which involves  $\text{HNO}_3$  leaching,  $\text{CH}_2\text{Cl}_2$  extraction, ethylation, trapping on a Tenax trap, isothermal GC separation, and quantification by cold vapor atomic fluorescence spectroscopy (CVAFS). The method detection limit for MeHg measurement was  $0.02\text{ ng g}^{-1}$ . The reproducibility, reported as RPDs, of MeHg measurement was  $<12\%$  (avg. RPD =  $8.8\%$ ). The extraction efficiencies for MeHg samples, using the spike method, were in

the range of  $85\text{--}113\%$ . A standard reference material ([MeHg] =  $75 \pm 4\text{ ng g}^{-1}$ , ERM-CC580 from the Institute for Reference Materials and Measurements of the European Commission) was interspersed with every 3 samples for quality control. The accuracy of MeHg measurement, assessed by measuring ERM standard reference material, was found to be less than  $9\%$  (RPDs), and the recoveries for ERM ranged from  $81\%$  to  $115\%$ . All results of  $\text{Hg}_T$  and MeHg concentrations are reported based on the dry weight of cryoconite samples.

For measurement of total organic carbon (TOC), the freeze-dried cryoconite samples were rinsed with  $10\%$  (v/v) aqueous HCl solution for 24 h to remove inorganic carbon present in the form of carbonates. The carbonate-free samples were then dried at  $40\text{ }^{\circ}\text{C}$  for 48 h. TOC was measured on a CHN elemental analyzer (PerkinElmer, model 2400; Boston, MA) by measuring the percent loss of weight on ignition. Replicate measurements of TOC were performed in standard reference material (dark brown soil,  $[\text{TOC}] = 1.8\%$ , GBW07401 from the Institute of Geophysical and Geochemical Exploration, China). The accuracy of TOC assessed by measuring GBW07401 standard reference material measurement was less than  $3\%$  (RPDs). The recoveries were in the range of  $95\text{--}105\%$ , whereas the reproducibility of replicated measurements was better than  $5\%$ . The statistical summary of measured parameters for QA/QC are present in Table S1, and further details about the analytical methods for  $\text{Hg}_T$ , MeHg, and TOC can be found elsewhere.<sup>21,30</sup>

## RESULTS AND DISCUSSION

**Distribution of  $\text{Hg}_T$  in Glacier Cryoconite in Western China.** As shown in Table 2, the  $\text{Hg}_T$  concentrations in glacier cryoconite varied from  $17.9$  to  $114.5\text{ ng g}^{-1}$  with a mean  $\pm$  standard deviation of  $52.7 \pm 25.6\text{ ng g}^{-1}$  ( $n = 48$ ). The average  $\text{Hg}_T$  concentrations were 1.4 times that of the values observed in topsoils (avg. =  $37.0\text{ ng g}^{-1}$ , range  $2.0\text{--}978.0\text{ ng g}^{-1}$ )<sup>31</sup> and sediments (avg. =  $36.0\text{ ng g}^{-1}$ , range  $7.6\text{--}119.8\text{ ng g}^{-1}$ )<sup>21</sup> in the Tibetan Plateau.

Spatially,  $\text{Hg}_T$  concentrations in cryoconite vary greatly among the glaciers, with those in the southern, monsoon-influenced region ( $66.0 \pm 29.3\text{ ng g}^{-1}$ ; including PL, YL, and ZD) being significantly higher ( $p = 0.004$ ,  $t$  test) than those in the northern, westerlies-influenced region ( $42.5 \pm 20.7\text{ ng g}^{-1}$ ; including TS, TGL, LHG, and SY). The highest concentrations were found in PL ( $84.0 \pm 1.7\text{ ng g}^{-1}$ ) and YL ( $81.2 \pm 17.6\text{ ng g}^{-1}$ ) in the southern region, which is about four times that in

**Table 2. Concentrations (Mean  $\pm$  Standard Deviation) of  $Hg_T$ , MeHg, and TOC in Cryoconite from Seven Glaciers in Western China**

sampling location	$Hg_T$ (ng g <sup>-1</sup> )	MeHg (ng g <sup>-1</sup> )	MeHg/ $Hg_T$ (%)	TOC (%)
Westerlies-influenced region				
TS	65.2 $\pm$ 12.5	1.1 $\pm$ 0.6	1.9 $\pm$ 1.5	3.1 $\pm$ 0.8
LHG	30.2 $\pm$ 8.2	0.9 $\pm$ 0.5	3.5 $\pm$ 2.4	1.6 $\pm$ 0.5
SY	20.0 $\pm$ 3.4	1.0 $\pm$ 0.3	5.3 $\pm$ 1.5	1.0 $\pm$ 0.2
TGL	31.5 $\pm$ 6.1	1.0	3.5	2.8 $\pm$ 0.2
region total	42.5 $\pm$ 20.7	1.0 $\pm$ 0.4	3.7 $\pm$ 2.1	2.2 $\pm$ 1.0
Monsoon-influenced region				
ZD	71.3 $\pm$ 1.2			7.3 $\pm$ 0.2
PL	84.0 $\pm$ 1.7			9.9 $\pm$ 0.1
YL	81.2 $\pm$ 17.6	0.9 $\pm$ 0.4	1.2 $\pm$ 0.6	9.7 $\pm$ 1.1
region total	66.0 $\pm$ 29.3	0.9 $\pm$ 0.4	1.2 $\pm$ 0.6	9.4 $\pm$ 1.3
Western China total	52.7 $\pm$ 25.6	1.0 $\pm$ 0.4	3.0 $\pm$ 2.1	4.2 $\pm$ 3.4

SY glacier cryoconite ( $20.0 \pm 3.4$  ng g<sup>-1</sup>) in the northern region.

The chemical composition of cryoconite is largely affected by the accumulation of atmospheric loadings,<sup>4–6</sup> which is especially the case in this study as our study sites are located far away from point sources of anthropogenic Hg emission. The northern and southern regions in this study are divided by the northern boundary of the Indian monsoon (Figure 1), which is generally defined based on seasonal changes in  $\delta^{18}O$  of precipitation on the Tibetan Plateau.<sup>20</sup> Earlier studies have indicated that the Indian monsoon carries large amounts of anthropogenic pollutants emitted by industrial and domestic activities from South Asia to Western China.<sup>19,32</sup> In contrast, the westerlies bring relatively less contaminants as they originate and travel far away from the upwind sources such as Europe and the Middle East.<sup>20,33</sup> This could explain why higher Hg concentrations occur in cryoconite in the southern glaciers, monsoon-influenced region (Table 2). This is further supported by the following observations. (1) Total gaseous Hg (TGM) concentrations are significantly greater in the southern region (e.g., 3.90 ng m<sup>-3</sup> at Mt. Gongga) than those in the northern region (e.g., 1.98 ng m<sup>-3</sup> at Mt. Waliguan).<sup>34</sup> The high levels of TGM in the southern region could favor the atmospheric Hg deposition and subsequent uptake of Hg by cryoconite. (2) Atmospheric deposition of Hg over the Tibetan Plateau occurs primarily via scavenging of particulate-bound Hg ( $Hg_p$ ) in the atmosphere,<sup>12,22</sup> and the rainfall amount was the governing factor affecting wet Hg deposition flux.<sup>23,35</sup> The glaciers in the southern region receive more rainfall (Table 1) and thus likely more scavenging and wet Hg deposition. (3) The landscape of the southern region is characterized by a frost cover, and cryoconite in the southern glaciers has higher airborne organic matter which is known to bind strongly with Hg.<sup>36</sup> This is demonstrated by a significant positive correlation ( $r = 0.91$ ;  $p < 0.001$ ) between  $Hg_T$  and TOC in the cryoconite (Figure 2) as well as high TOC and elevated Hg levels in the southern region (Table 2).

Altitudinally, with an increasing elevation  $Hg_T$  concentrations in glacier cryoconite decrease significantly ( $r = 0.55$ ;  $p < 0.001$ ) in the northern region (Figure 3a). As pointed out above, Hg in cryoconite could be largely attributed to  $Hg_p$  as atmospheric Hg deposition on the glaciers over Western China

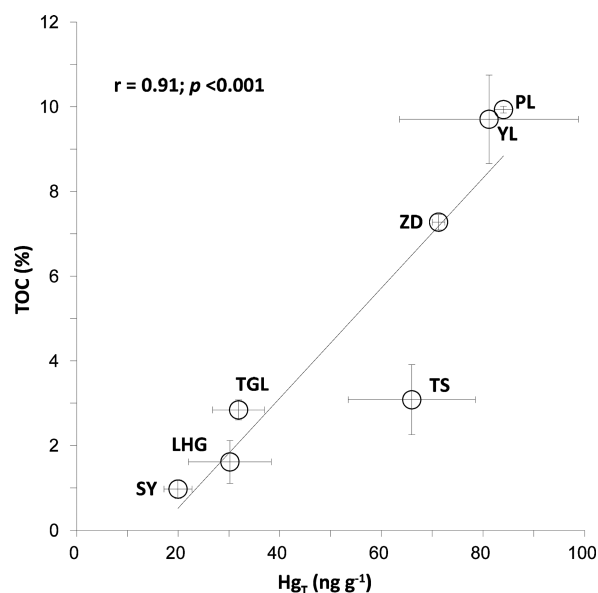


**Figure 2.** Relationship between  $Hg_T$  and TOC in Glacier Cryoconite collected from various glaciers in Western China (circle represents the site with the center representing mean values of TOC and  $Hg_T$ , whereas standard deviations (1SD) are represented by vertical and horizontal error bars, respectively. Sites influenced by Indian monsoon and Westerlies are also shown with the oval).

was primarily associated with particulate matter. Mineral dust is the main component of atmospheric particulate matter,<sup>37</sup> and its deposition generally decreases as altitude increases over Western China.<sup>38</sup> In addition, the melting process also favors the accumulation of Hg in cryoconite at lower altitudes. The cryoconite samples in this study were collected in the ablation zone (Table 1), which is prone to a glacier melting process below the equilibrium line altitude.<sup>39</sup> Glaciers at lower elevations undergo more intensive melting during the ablation season, resulting in more accumulation of particulate matter and associated  $Hg_p$  from the melted layer and thus higher Hg concentration in cryoconite.<sup>39–41</sup> Several previous studies have indicated that solute elution is a common process associated with the snow/ice melt period,<sup>42,43</sup> which may also affect the Hg accumulation in cryoconite. However, no information is available at this time on the solubility and solid state diffusion coefficient of Hg in cryoconite and snow/ice; thus, we are not able to assess the magnitude of Hg released via these processes in this study. In contrast,  $Hg_T$  concentrations in cryoconite did not show any statistically significant variation with altitude ( $r = 0.14$ ;  $p = 0.68$ ) in the southern region (Figure 3b). This could be due to the altitudinal distribution of TOC in the southern glaciers, although cryoconite samples from the monsoon-influenced region is much less populated and unbalanced sample numbers might result in the absence of some of these statistical relationships, especially PL and ZD glaciers ( $n = 2$ , Table 1). For each individual glacier (Figure S2, Supporting Information), YL is the only glacier where TOC increases significantly with  $Hg_T$  ( $r = 0.61$ ,  $p < 0.05$ ). This might explain why the altitudinal pattern of cryoconite Hg in the southern region behaves differently from the northern region (Figure 2b). We should however point out that TOC at large spatial scale is positively correlated with  $Hg_T$  as discussed earlier (Figure 2).

**Cryoconite as a Potential Site for Hg Methylation.** MeHg concentrations in cryoconite varied from 0.4 to 1.7 ng

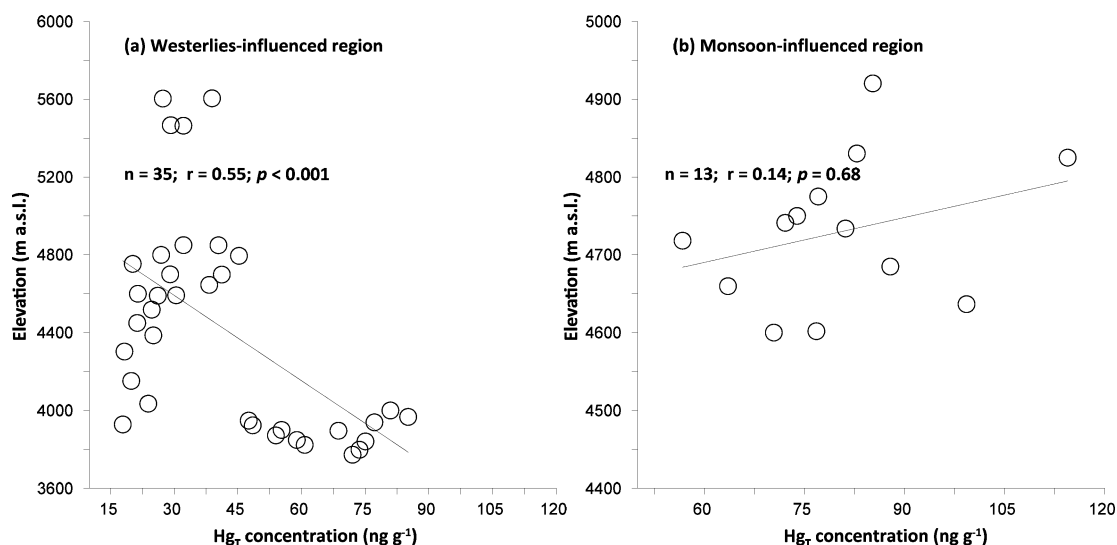


**Figure 3.** Relationships between Hg<sub>T</sub> concentrations in cryoconite and elevations of glaciers from the northern (a) and southern (b) regions in Western China.

g<sup>-1</sup> with an average of  $1.0 \pm 0.4 \text{ ng g}^{-1}$  (Table 2). The percentage of Hg<sub>T</sub> present as MeHg (MeHg%) varied from 0.7% to 7.0% with a mean of  $3.0\% \pm 2.1\%$ . Different from Hg<sub>T</sub>, there was no significant regional or altitudinal pattern in either MeHg concentration or MeHg% in cryoconite samples collected from the study region (Figure S3, Supporting Information). However, MeHg concentrations in cryoconite are several orders of magnitude higher than those reported for topsoils over the Tibetan Plateau ( $0.002\text{--}0.058 \text{ ng g}^{-1}$ )<sup>44</sup> and are comparable with the values reported in sediments ( $0.543\text{--}1.133 \text{ ng g}^{-1}$ ),<sup>30,45</sup> mosses (avg. =  $1.1 \text{ ng g}^{-1}$ ), and lichens (avg. =  $1.5 \text{ ng g}^{-1}$ )<sup>46</sup> from this region. The average MeHg% was also markedly higher than the values observed in precipitation<sup>23</sup> and soils<sup>30</sup> in the Tibetan Plateau. Although trace amounts of MeHg can be present in the atmospheric boundary layer,<sup>47</sup> they are unlikely sufficient to account for the high MeHg concentrations in cryoconite.

Our results represent the first report on MeHg in cryoconite, revealing that cryoconite on high-elevation glaciers under low temperatures could be a new, previously unknown site for Hg methylation. This is very likely possible as cryoconite is known to host active microbial communities.<sup>3</sup> The recurring freeze–thaw cycles of cryoconite on alpine glaciers of Western China may favor methylation of the newly deposited Hg(II).<sup>48,49</sup> A similar Hg methylation in marine cryospheric environments such as sea ice has also been proposed.<sup>50,51</sup> Further studies are needed to explore the methylation mechanism in glacier cryoconite.

**Implications for Hg Accumulation in Glaciers of Western China.** The cryoconite formation process occurs only during the glacier melting season, and the formed cryoconite can be stored into the glacier as well as released into downstream ecosystems with meltwater. After the ablation season, glacier surfaces will be covered with frequent and heavy snowfall and receive new cryoconite deposition. When the glacier surfaces start melting again in the next year, the cryoconite steps into a new period of the formation process and Hg accumulation. Given the cryoconite has potential for Hg methylation and that cryoconite is widespread on alpine glaciers across Western China during the ablation season,<sup>52</sup> they can serve as an important reservoir for Hg and MeHg

accumulation. This can be clearly seen in our study, reflecting high Hg and MeHg concentrations in glacier cryoconite in Western China. Therefore, we made a primary attempt to estimate the potential contribution of cryoconite-related Hg to the glacier reservoir by using the following simple equation

$$P = C_{\text{Hg}} \times W \times F \times S \quad (1)$$

where  $P$  is approximately the annual amount of Hg stored in cryoconite (kilograms per a single year of formation process),  $C_{\text{Hg}}$  is the concentration of Hg in cryoconite ( $\text{ng g}^{-1}$ ),  $W$  is the mass of cryoconite per square meter ( $\text{g m}^{-2}$ ),  $F$  is the fraction of cryoconite coverage on glacier surfaces (%), and  $S$  is the total glacier surface area in Western China ( $\text{m}^2$ ). The average concentrations of Hg<sub>T</sub> and MeHg in cryoconite were taken as  $52.7 \pm 25.6$  and  $0.96 \pm 0.41 \text{ ng g}^{-1}$ , respectively, as observed in this study (Table 2). The total area of glaciers in Western China is estimated to be  $43\,087 \text{ km}^2$ , and the ablation zone area on the glaciers is assumed to be one-third of the total glacier area.<sup>16</sup> The fraction of cryoconite coverage on the glacier surface in Western China is not known very accurately; therefore, we used a value of 6%, which is the highest reference value reported for polar glaciers.<sup>24</sup> The mass of cryoconite per square meter on the glaciers over Western China was estimated from the average of reported values from Altai ( $123 \text{ g m}^{-2}$ ),<sup>53</sup> Himalayas ( $300 \text{ g m}^{-2}$ ),<sup>54</sup> Qilian ( $292 \text{ g m}^{-2}$ ),<sup>55</sup> and Tianshan Mountains ( $334 \text{ g m}^{-2}$ ).<sup>56</sup> With these assumptions, the annual amounts of Hg<sub>T</sub> and MeHg stored in glacier cryoconite over Western China were estimated to be  $34.3 \pm 17.4$  and  $0.65 \pm 0.28 \text{ kg}$  from a single year of formation process, respectively. It is pertinent to state that our regional estimates of the Hg amount stored in cryoconite are likely to have significant uncertainty due to the assumption and values used in the calculation. For example, our estimation is from a relatively small number of glaciers (only 7 out of 42 370 glaciers), and thus, Hg<sub>T</sub> and MeHg concentration in cryoconite may not be representative of the entire glacier cryoconite of Western China. In addition, the fraction of cryoconite coverage on glacier surfaces ( $F$ ) is taken from the polar glaciers and thus may not be a true representative of glacier cryoconite coverage of Western China. Our own field experience shows that the percent of cryoconite coverage could be more than

6%, and thus, the annual amount of Hg stored in cryoconite represents only a lower bound. Nonetheless, our study provides the first report on Hg<sub>T</sub> and MeHg stored in the glaciers in cryoconite in a single year of formation process from Western China.

Photoreduction and demethylation are important processes which could result in loss of Hg<sub>T</sub> and MeHg from glacial systems. However, an earlier study<sup>57</sup> suggested that snow Hg in Western China was less influenced by the effect of postdepositional processes (e.g., reemission, photoreduction) than in the polar regions (e.g., 31% loss in Tibetan surface snow vs 92% loss of Hg in Arctic surface snow). This indicated that the loss of Hg<sub>T</sub> and MeHg in cryoconite by photoreduction and demethylation processes would be lower over Western China, and thus, the annual amount of Hg stored in cryoconite is expected to be larger in our study due to several reasons. First, the fraction of cryoconite coverage on the glacier surface in Western China is expected to be much higher than 6% due to the large arid and semiarid areas around these glaciers (Figure 1). Second, the ablation area of a glacier undergoes cryoconite formation and redistribution many times during the ablation season. Moreover, the settling of particulate matter may lead to the removal of Hg from the uppermost layers of snow/ice during the melting period,<sup>39–41</sup> which could transport cryoconite Hg to the lower strata when cryoconite moves downward. This also suggests that a large amount of cryoconite Hg could have been historically accumulated inside glaciers over Western China.

Glaciers are known to act as a temporary storage reservoir for Hg. For instance, Zhang et al.<sup>40</sup> estimated that ~2500 kg of Hg has been released over the past 40 years at an average rate of 62.5 kg year<sup>-1</sup> from glaciers in Western China. However, this estimate considered only the melting of snow/ice and did not include the contribution of cryoconite which has been suggested to have strong abilities in Hg accumulation. Therefore, our study indicates that the temporary storage and release of Hg in glaciers could be larger than the previous estimates.<sup>40</sup> Together with the considerable concentrations of Hg and relatively high MeHg/Hg<sub>T</sub> ratios found in cryoconite, our study highlights the importance of cryoconite in Hg storage and transformation in glaciers over Western China. More importantly, as a result of the rapid climate warming, more extensive recession of glaciers over Western China has become inevitable in the foreseeable future.<sup>58</sup> The total amount of released Hg is expected to increase under the global warming scenario in the future. It is also important to note that melting of glaciers is the major source of freshwater for downstream regions.<sup>18</sup> It is, thus, reasonable to expect that the historically accumulated cryoconite Hg may be released during melting of these glaciers. The accelerated melting of glaciers not only acts as an important source of water but also acts as Hg and MeHg contaminants, which could be subsequently released and may contaminate downstream ecosystems. Further studies are needed to better quantify the storage, fate, and transport of Hg and to elucidate the Hg methylation process in cryoconite to fully understand the implications of cryoconite Hg for biogeochemical Hg cycling in the regional and global cryosphere under rapid climate warming.

## ■ ASSOCIATED CONTENT

### § Supporting Information

The Supporting Information is available free of charge on the ACS Publications website at DOI: 10.1021/acs.est.8b06575.

Details about the cryoconite sample collection and study area; photos showing the cryoconite on the alpine glacier surface in the ablation zone during the summer ablation season; individual correlation between Hg<sub>T</sub> concentration and TOC content for YL, LHG, TS, SY, TGL glaciers; variations of MeHg concentrations and MeHg% in cryoconite with increasing altitude; statistics of measured parameters for analytical procedures and QA/QC; references (PDF)

## ■ AUTHOR INFORMATION

### Corresponding Author

\*E-mail: [huangjie@itpcas.ac.cn](mailto:huangjie@itpcas.ac.cn). Tel/Fax: +86-10-80497034.

### ORCID

Jie Huang: 0000-0002-3060-0862

Zhiyuan Cong: 0000-0002-7545-5611

Jianzhong Xu: 0000-0002-9933-1744

Feiyue Wang: 0000-0001-5297-0859

### Notes

The authors declare no competing financial interest.

## ■ ACKNOWLEDGMENTS

We are grateful to Yajun Liu, Yang Li, and Xiaofei Li for their arduous fieldwork for cryoconite sampling. We also very much appreciate the three reviewers' insightful comments and suggestions on the paper. This research was supported by the National Natural Science Foundation of China (Grant Nos. 41571073, 41522103, and 41421061), the Strategic Priority Research Program (A) of the Chinese Academy of Sciences (CAS), Pan-Third Pole Environment Study for a Green Silk Road (Pan-TPE) (XDA20040501), the Foundation of State Key Laboratory of Cryospheric Science, CAS (Grant No. SKLCS-ZZ-2019), the Youth Innovation Promotion Association, CAS (2018094), and the Canada Research Chairs program. R.Y. was funded by the Chinese Academy of Sciences through the Pioneer Hundred Talent Plan. K.R. thanks Banaras Hindu University for granting the study leave and CAS for international visiting scholar support under the PIFI program (2018VCC0005).

## ■ REFERENCES

- (1) Cook, J.; Edwards, A.; Takeuchi, N.; Irvine-Fynn, T. Cryoconite: The dark biological secret of the cryosphere. *Prog. Phys. Geog.* **2016**, *40*, 66–111.
- (2) Wientjes, I. G. M.; Van de Wal, R. S. W.; Reichert, G. J.; Sluijs, A.; Oerlemans, J. Dust from the dark region in the western ablation zone of the Greenland ice sheet. *Cryosphere* **2011**, *5*, 589–601.
- (3) Stibal, M.; Šabacká, M.; Žárský, J. Biological processes on glacier and ice sheet surfaces. *Nat. Geosci.* **2012**, *5*, 771–774.
- (4) Singh, S. M.; Sharma, J.; Gawas-Sakhalkar, P.; Upadhyay, A. K.; Naik, S.; Pedneker, S. M.; Ravindra, R. Atmospheric deposition studies of heavy metals in Arctic by comparative analysis of lichens and cryoconite. *Environ. Monit. Assess.* **2013**, *185*, 1367–1376.
- (5) Singh, S. M.; Avinash, K.; Sharma, P.; Mulik, R. U.; Upadhyay, A. K.; Ravindra, R. Elemental variations in glacier cryoconites of Indian Himalaya and Spitsbergen, Arctic. *Geosci. Front.* **2017**, *8*, 1339–1347.
- (6) Łokas, E.; Zaborska, A.; Kolicka, M.; Różycki, M.; Zawierucha, K. Accumulation of atmospheric radionuclides and heavy metals in

cryoconite holes on an Arctic glacier. *Chemosphere* **2016**, *160*, 162–172.

(7) Driscoll, C. T.; Mason, R. P.; Chan, H. M.; Jacob, D. J.; Pirrone, N. Mercury as a global pollutant: sources, pathways, and effects. *Environ. Sci. Technol.* **2013**, *47*, 4967–4983.

(8) Mergler, D.; Anderson, H. A.; Chan, L. H. M.; Mahaffey, K. R.; Murray, M.; Sakamoto, M.; Stern, A. H. Methylmercury exposure and health effects in humans: a worldwide concern. *Ambio* **2007**, *36*, 3–11.

(9) Selin, H. Global environmental law and treaty-making on hazardous substances: the Minamata Convention and mercury abatement. *Global Environ. Polit.* **2014**, *14*, 1–19.

(10) Lindeberg, C.; Bindler, R.; Bigler, C.; Rosén, P.; Renberg, I. Mercury pollution trends in subarctic lakes in northern Swedish mountains. *Ambio* **2007**, *36*, 401–405.

(11) Zheng, J. Archives of total mercury reconstructed with ice and snow from Greenland and the Canadian High Arctic. *Sci. Total Environ.* **2015**, *509–510*, 133–144.

(12) Loewen, M.; Kang, S.; Armstrong, D.; Zhang, Q.; Tomy, G.; Wang, F. Atmospheric transport of mercury to the Tibetan Plateau. *Environ. Sci. Technol.* **2007**, *41*, 7632–7638.

(13) Yang, H.; Battarbee, R. W.; Turner, S. D.; Rose, N. L.; Derwent, R. G.; Wu, G.; Yang, R. Historical reconstruction of mercury pollution across the Tibetan Plateau using lake sediments. *Environ. Sci. Technol.* **2010**, *44*, 2918–2924.

(14) Yao, T.; Thompson, L.; Yang, W.; Yu, W.; Gao, Y.; Guo, X.; Yang, X.; Duan, K.; Zhao, H.; Xu, B. Different glacier status with atmospheric circulations in Tibetan Plateau and surroundings. *Nat. Clim. Change* **2012**, *2*, 663–667.

(15) Jacob, T.; Wahr, J.; Pfeffer, W. T.; Swenson, S. Recent contributions of glaciers and ice caps to sea level rise. *Nature* **2012**, *482*, 514–518.

(16) Guo, W.; Liu, S.; Xu, J.; Wu, L.; Shangguan, D.; Yao, X.; Wei, J.; Bao, W.; Yu, P.; Liu, Q.; Jiang, Z. The second Chinese glacier inventory: data, methods and results. *J. Glaciol.* **2015**, *61*, 357–372.

(17) Pfeffer, W. T.; Arendt, A. A.; Bliss, A.; Bolch, T.; Cogley, J. G.; Gardner, A. S.; Hagen, J.; Hock, R.; Kaser, G.; Christian, K.; Evan, S. M.; Geir, M.; Nico, M.; Frank, P.; Valentina, R.; Philipp, R.; Bruce, H. R.; Justin, R.; Martin, J. S.; Consortium, T. R. The Randolph glacier inventory: a globally complete inventory of glaciers. *J. Glaciol.* **2014**, *60*, 537–552.

(18) Immerzeel, W. W.; Van Beek, L. P. H.; Bierkens, M. F. P. Climate change will affect the Asian water towers. *Science* **2010**, *328*, 1382–1385.

(19) Lüthi, Z. L.; Škerlak, B.; Kim, S. W.; Lauer, A.; Mues, A.; Rupakheti, M.; Kang, S. Atmospheric Brown Clouds reach the Tibetan Plateau by crossing the Himalayas. *Atmos. Chem. Phys.* **2015**, *15*, 6007–6021.

(20) Xu, B.; Cao, J.; Hansen, J.; Yao, T.; Joswia, D. R.; Wang, N.; Wu, G.; Wang, M.; Zhao, H.; Yang, W. Black soot and the survival of Tibetan glaciers. *Proc. Natl. Acad. Sci. U. S. A.* **2009**, *106*, 22114–22118.

(21) Kang, S.; Huang, J.; Wang, F.; Zhang, Q.; Zhang, Y.; Li, C.; Wang, L.; Chen, P.; Sharma, C. M.; Li, Q. Atmospheric mercury depositional chronology reconstructed from lake sediments and ice core in the Himalayas and Tibetan Plateau. *Environ. Sci. Technol.* **2016**, *50*, 2859–2869.

(22) Huang, J.; Kang, S.; Guo, J.; Zhang, Q.; Xu, J.; Jenkins, M.; Zhang, G.; Wang, K. Seasonal variations, speciation and possible sources of mercury in the snowpack of Zhadang glacier, Mt. Nyainqentanglha, southern Tibetan Plateau. *Sci. Total Environ.* **2012**, *429*, 223–230.

(23) Huang, J.; Kang, S.; Zhang, Q.; Yan, H.; Guo, J.; Jenkins, M. G.; Zhang, G.; Wang, K. Wet deposition of mercury at a remote site in the Tibetan Plateau: Concentrations, speciation, and fluxes. *Atmos. Environ.* **2012**, *62*, 540–550.

(24) Sävström, C.; Mumford, P.; Marshall, W.; Hodson, A.; Laybourn-Parry, J. The microbial communities and primary

productivity of cryoconite holes in an Arctic glacier (Svalbard 79°N). *Polar Biol.* **2002**, *25*, 591–596.

(25) Edwards, A.; Pachebat, J.; Swain, M.; Hegarty, M.; Hodson, A.; Irvine-Fynn, T.; Rassner, S.; Sattler, B. A metagenomic snapshot of taxonomic and functional diversity in an alpine glacier cryoconite ecosystem. *Environ. Res. Lett.* **2013**, *8*, 035003.

(26) Baccolo, G.; Di Mauro, B.; Massabò, D.; Clemenza, M.; Nastasi, M.; Delmonte, B.; Prata, M.; Prati, P.; Previtali, E.; Maggi, V. Cryoconite as a temporary sink for anthropogenic species stored in glaciers. *Sci. Rep.* **2017**, *7*, 9623 DOI: 10.1038/s41598-017-10220-5.

(27) Yanai, M.; Wu, G. X. Effects of the Tibetan Plateau. In *The Asian Monsoon*; Springer: Berlin, 2005; pp 513–549.

(28) Dong, Z.; Kang, S.; Qin, D.; Li, Y.; Wang, X.; Ren, J.; Li, X.; Yang, J.; Qin, X. Provenance of cryoconite deposited on the glaciers of the Tibetan Plateau: New insights from Nd-Sr isotopic composition and size distribution. *J. Geophys. Res.* **2016**, *121*, 7371–7382.

(29) Liang, L.; Horvat, M.; Feng, X.; Shang, L.; Li, H.; Pang, P. Re-evaluation of distillation and comparison with HNO<sub>3</sub> leaching/solvent extraction for isolation of methylmercury compounds from sediment/soil samples. *Appl. Organomet. Chem.* **2004**, *18*, 264–270.

(30) Ma, M.; Du, H.; Wang, D.; Kang, S.; Sun, T. Biotically mediated mercury methylation in the soils and sediments of Nam Co Lake, Tibetan Plateau. *Environ. Pollut.* **2017**, *227*, 243–251.

(31) Sheng, J.; Wang, X.; Gong, P.; Tian, L.; Yao, T. Heavy metals of the Tibetan top soils. *Environ. Sci. Pollut. Res.* **2012**, *19*, 3362–3370.

(32) Cong, Z.; Kawamura, K.; Kang, S.; Fu, P. Penetration of biomass-burning emissions from South Asia through the Himalayas: new insights from atmospheric organic acids. *Sci. Rep.* **2015**, *5*, 9580.

(33) Wang, X.; Gong, P.; Wang, C.; Ren, J.; Yao, T. A review of current knowledge and future prospects regarding persistent organic pollutants over the Tibetan Plateau. *Sci. Total Environ.* **2016**, *573*, 139–154.

(34) Fu, X.; Feng, X.; Sommar, J.; Wang, S. A review of studies on atmospheric mercury in China. *Sci. Total Environ.* **2012**, *421*, 73–81.

(35) Huang, J.; Kang, S.; Zhang, Q.; Guo, J.; Sillanpää, M.; Wang, Y.; Sun, S.; Sun, X.; Tripathee, L. Characterizations of wet mercury deposition on a remote high-elevation site in the southeastern Tibetan Plateau. *Environ. Pollut.* **2015**, *206*, 518–526.

(36) Ravichandran, M. Interactions between mercury and dissolved organic matter—a review. *Chemosphere* **2004**, *55*, 319–331.

(37) Wake, C. P.; Dibb, J. E.; Mayewski, P. A.; Zhongqin, L.; Zichu, X. The chemical composition of aerosols over the Eastern Himalayas and Tibetan plateau during low dust periods. *Atmos. Environ.* **1994**, *28*, 695–704.

(38) Wu, G.; Yao, T.; Xu, B.; Tian, L.; Zhang, C.; Zhang, X. Dust concentration and flux in ice cores from the Tibetan Plateau over the past few decades. *Tellus, Ser. B* **2010**, *62*, 197–206.

(39) Huang, J.; Kang, S.; Guo, J.; Sillanpää, M.; Zhang, Q.; Qin, X.; Du, W.; Tripathee, L. Mercury distribution and variation on a high-elevation mountain glacier on the northern boundary of the Tibetan Plateau. *Atmos. Environ.* **2014**, *96*, 27–36.

(40) Zhang, Q.; Huang, J.; Wang, F.; Loewen, M.; Xu, J.; Armstrong, D.; Li, C.; Zhang, Y.; Kang, S. Mercury distribution and deposition in glacier snow over western China. *Environ. Sci. Technol.* **2012**, *46*, 5404–5413.

(41) Witherow, R. A.; Lyons, W. B. Mercury deposition in a polar desert ecosystem. *Environ. Sci. Technol.* **2008**, *42*, 4710–4716.

(42) Tranter, M.; Brimblecombe, P.; Davies, T. D.; Vincent, C. E.; Abrahams, P. W.; Blackwood, I. The composition of snowfall, snowpack and meltwater in the Scottish highlands—evidence for preferential elution. *Atmos. Environ.* **1986**, *20*, 517–525.

(43) Dommergue, A.; Ferrari, C. P.; Gauchard, P. A.; Boutron, C. F.; Poissant, L.; Pilote, M.; Jitaru, P.; Adams, F. C. The fate of mercury species in a sub-arctic snowpack during snowmelt. *Geophys. Res. Lett.* **2003**, *30*(1621), DOI: 10.1029/2003GL017308.

(44) Liu, Y.; Dong, J.; Zhang, Q.; Wang, J.; Han, L.; Zeng, J.; He, J. Longitudinal occurrence of methylmercury in terrestrial ecosystems of the Tibetan Plateau. *Environ. Pollut.* **2016**, *218*, 1342–1349.

(45) Xu, X.; Zhang, Q.; Wang, W. Linking mercury, carbon, and nitrogen stable isotopes in Tibetan biota: Implications for using mercury stable isotopes as source tracers. *Sci. Rep.* **2016**, *6*, 25394.

(46) Shao, J.; Liu, C.; Zhang, Q.; Fu, J.; Yang, R.; Shi, J.; Cai, Y.; Jiang, G. Characterization and speciation of mercury in mosses and lichens from the high-altitude Tibetan Plateau. *Environ. Geochem. Health* **2017**, *39*, 475–482.

(47) Baya, P. A.; Gosselin, M.; Lehnher, I.; St. Louis, V. L.; Hintelmann, H. Determination of monomethylmercury and dimethylmercury in the Arctic marine boundary layer. *Environ. Sci. Technol.* **2015**, *49*, 223–232.

(48) Renner, R. Newly deposited mercury may be more bioavailable. *Environ. Sci. Technol.* **2002**, *36*, 226A–227A.

(49) O'Concubhair, R.; O'Sullivan, D.; Sodeau, J. R. Dark oxidation of dissolved gaseous mercury in polar ice mimics. *Environ. Sci. Technol.* **2012**, *46*, 4829–4836.

(50) Beattie, S. A.; Armstrong, D.; Chaulk, A.; Comte, J.; Gosselin, M.; Wang, F. Total and methylated mercury in Arctic multiyear sea ice. *Environ. Sci. Technol.* **2014**, *48*, 5575–5582.

(51) Gionfriddo, C. M.; Tate, M. T.; Wick, R. R.; Schultz, M. B.; Zemla, A.; Thelen, M. P.; Schofield, R.; Krabbenhoft, D. P.; Holt, K. E.; Moreau, J. W. Microbial mercury methylation in Antarctic sea ice. *Nat. Microbio.* **2016**, *1*, 16127.

(52) Nagatsuka, N.; Takeuchi, N.; Nakano, T.; Shin, K.; Kokado, E. Geographical variations in Sr and Nd isotopic ratios of cryoconite on Asian glaciers. *Environ. Res. Lett.* **2014**, *9*, 045007.

(53) Takeuchi, N.; Uetake, J.; Fujita, K.; Aizen, V.; Nikitin, S. A snow algal community on Akkem Glacier in the Russian Altai Mountains. *Ann. Glaciol.* **2006**, *43*, 378–384.

(54) Takeuchi, N.; Kohshima, S.; Seko, K. Structure, formation, and darkening process of albedo-reducing material (Cryoconite) on a Himalayan glacier: a granular algal mat growing on the Glacier. *Arct. Antarct. Alp. Res.* **2001**, *33*, 115–122.

(55) Takeuchi, N.; Matsuda, Y.; Sakai, A.; Fujita, K. A large amount of biogenic surface dust (cryoconite) on a glacier in the Qilian Mountains, China. *Bull. Glaciol. Res.* **2005**, *22*, 1–8.

(56) Takeuchi, N.; Li, Z. Characteristics of surface dust on Ürümqi glacier No. 1 in the Tien Shan mountains, China. *Arct. Antarct. Alp. Res.* **2008**, *40* (4), 744–750.

(57) Huang, J.; Kang, S.; Zhang, Q.; Jenkins, M.; Guo, J.; Zhang, G.; Wang, K. Spatial distribution and magnification processes of mercury in snow from high-elevation glaciers in the Tibetan Plateau. *Atmos. Environ.* **2012**, *46*, 140–146.

(58) Shi, Y.; Liu, S. Estimation on the response of glaciers in China to the global warming in the 21st century. *Chin. Sci. Bull.* **2000**, *45*, 668–672.